Journal of Organometallic Chemistry, 393 (1990) 315–331
Elsevier Sequoia S.A., Lausanne
JOM 20926

The coordination modes of simple diarylmagnesium species: some representative X-ray crystal structures

Peter R. Markies, Gerrit Schat, Otto S. Akkerman, Friedrich Bickelhaupt *,
Scheikundig Laboratorium, Vrije Universiteit, De Boelelaan 1083, 1081 HV Amsterdam (The Netherlands)

Wilberth J.J. Smeets, Paul van der Sluis, and Anthony L. Spek
Vakgroep Algemene Chemie, Afdeling Kristal- en Structuurchemie, University of Utrecht, Padualaan 8, 3584 CH Utrecht (The Netherlands)

(Received March 7th, 1990)

Abstract

The coordination modes of simple diarylmagnesium species have been investigated by crystal structure studies of representation compounds. In the case of diphenylmagnesium (**1**), both the solvated monomeric complex $Ph_2Mg \cdot [THF]_2$ (**1a**) and the solvent-free compound $[Ph_2Mg]_n$ (**1b**) were characterized. A polymeric structure was found for **1b**, with tetrahedrally coordinated magnesium atoms interconnected by μ,η^1-bridging phenyl groups to form linear chains. Bis(*p*-tolyl)magnesium (**3**) crystallized in a remarkable double structure that contained dimeric and monomeric units in a 1:2 ratio. In the dimer, two aryl groups are μ,η^1-bridging.

Introduction

In earlier investigations, we studied the complexation of diphenylmagnesium (**1**) with some crown ether ligands. A remarkable crystal structure was found for the complex [1,3-xylyl-18-crown-5] · $[Ph_2Mg]$ (**2**), which has a rotaxane or threaded structure [1]. In **2**, an approximately linear Ph–Mg–Ph unit is equatorially surrounded by four of the five crown ether oxygen atoms. With the analogous, but smaller crown ether 1,3-xylyl-15-crown-4, a remarkable metallation reaction occurred [2]. This reaction, which is unusual in organomagnesium chemistry, probably starts with formation of a crown ether/diorganylmagnesium complex, which cannot be isolated because it reacts further. (The complexation of **1** with glymes is also being investigated, and the crystal structures of these complexes will be reported separately.) The investigations had to be performed in diethyl ether, since in THF the strong donor ability of this solvent prevented formation of complexes with the

0022-328X/90/$03.50

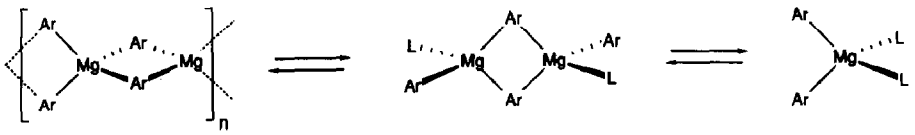

$[Ar_2Mg]_n$ $[Ar_2Mg.THF]_2$ $Ar_2Mg.[THF]_2$

Scheme 1

polyethers. Instead, the bis(tetrahydrofuran) complex was formed. Under suitable conditions, crystals of $Ph_2Mg \cdot [THF]$, (**1a**) were isolated [3].

Since, surprisingly, the crystal structure of compound **1a** has not previously been described, an X-ray diffraction study was performed. In studies of both inter- and intra-molecularly coordinated more complicated diphenylmagnesium complexes, the structure of **1a** will serve as a reference. There are no structural data on oligomeric diarylmagnesium compounds in the literature, justifying further experiments with **1** aimed at obtaining crystalline complexes of this type. In addition to **1**, related bis(*p*-tolyl)magnesium (**3**) was also investigated; because of the small differences in physical properties between **1** and **3**, the observations on these reagents were expected to be complementary. In solution, various aggregates are present in equilibrium, as depicted in Scheme 1. It seemed likely that, depending on the crystallization conditions, the monomeric, dimeric, or polymeric species could be isolated. Formation of the such species should be aided by use of a non-polar medium (low THF content) [4]. As in the case of dialkylmagnesium complexes, oligomerization of **1** and **3** might occur by bridging of the organic groups via three-center two-electron bonds involving two magnesium atoms [5].

Experimental

All manipulations involving diarylmagnesium compounds were performed in sealed glass apparatus by high vacuum techniques [6], since even small traces of impurities interfere with the crystallization. Twice- or triply-sublimed magnesium was used. THF, Et_2O, n-hexane and benzene were distilled from potassium/sodium alloy. ^1H and ^{13}C NMR spectra were recorded on a Bruker WM-250 spectrometer at 250 and 62.89 MHz, respectively. Melting points are uncorrected. The elemental analysis of **5** was carried out at the Organic Chemical Institute TNO, Zeist, The Netherlands. Concentrations of 'total base' and Mg^{2+} in organomagnesium solutions were determined by titration of a sample of known volume against acid or EDTA, respectively [6].

Diarylmercury compounds

Diphenylmercury (**4**) and bis(*p*-tolyl)mercury (**5**) were characterized by their ^1H and ^{13}C NMR spectra in THF-d_8, which were only slightly different from those obtained in other solvents [7,8]. Compound **5** was purified by high vacuum sublimation at 140 °C/10^{-2} mmHg; the identity of the colorless solid (m.p. 236–237 °C; lit. 238 [9] and 243 °C [7]) was checked by elemental analysis.

Diphenylmercury (4) (from Merck). ^1H NMR (250 MHz, ref. THF-d_7 = 1.75 ppm) δ 7.09–7.23 (m, 2H, aryl-H(3)), 7.25-7.50 (m, 3H, aryl-H(2,4)). ^{13}C NMR (62.89 MHz, ref. THF-d_8 = 24.0 ppm) δ 128.1 (dt, ^1J(C–H) = 159 Hz, ^3J(C–H) = 7

Hz, 2C, aryl-C(4)), 128.7 (dd, ^1J(C–H) = 158 Hz, ^3J(C–H) = 7 Hz, 4C, aryl-C(3)), 138.4 (ddd, ^1J(C–H) = 159 Hz, ^3J(C–H) = 8 Hz, ^3J(C–H) = 8 Hz, 4C, aryl-C(2)), 171.6 (s, 2C, aryl-C(1)).

Bis(p-tolyl)mercury (5). Found: C, 43.12; H, 3.69; Hg, 52.39. $C_{14}H_{14}Hg$ calc.: C, 43.92; H, 3.62; Hg, 51.33. Mass spectrum *m/z* (relative intensity): 384 (10), 182 (44), 167 (17), 65 (28), 39 (11), HRMS ($C_{14}H_{14}{}^{202}Hg$): found 384.0824, calc. 384.0802. ^{1}H NMR (250 MHz, ref. THF-d_7 = 1.75 ppm) δ 2.33 (s, 6H, Me), 7.17 (d, ^3J = 8 Hz, 4H, aryl-H(3)), 7.30 (d, ^3J = 8 Hz, 4 H, aryl-H(2)). ^{13}C NMR (62.89 MHz, ref. THF-d_8 = 24.0 ppm) δ 21.4 (q, ^1J(C–H) = 126 Hz, 2C, Me), 129.4 (d, ^1J(C–H) = 156 Hz, 4C, aryl-C(3)), 137.3 (dd, ^1J(C–H) = 159 Hz, ^3J(C–H) = 8 Hz, 4C, aryl-C(2)), 137.9 (s, 2C, aryl-C(4)), aryl-C(1) not found.

Diarylmagnesium compounds

Solutions of **1** and **3** in THF were prepared by stirring a mixture of the diaryl-mercury compound (**4** or **5**, 10 mmol), Mg metal (2.4 g, 100 mmol) and THF (100 mL) for two weeks at room temperature. After settling of the magnesium amalgam, the clear solution (yellowish brown) was decanted into another vessel. Completion of the reaction was checked by titration of an aliquot of known volume to determine the 'total base' and Mg^{2+} concentrations after hydrolysis [6]. The diarylmagnesium reagent solutions were divided between several ampoules (1 mmol, 10 mL THF) for the crystallizations.

The THF complexes of **1** and **3** crystallized upon cooling of a saturated solution (1 mmol) of the diarylmagnesium reagent in THF/n-hexane (1 : 10, 10 mL) slowly from r.t. to −20 °C. The colorless crystalline solid was isolated by decantation and pumping (10^{-3} mbar) to remove the last traces of free solvent. Some crystals were examined by ^{1}H NMR and ^{13}C NMR spectroscopy to check their identity. Crystals suitable for an X-ray structure determination were selected in a nitrogen-filled glovebox (less than 1 ppm H_2O and O_2). The remaining material was hydrolyzed and 'total base' and Mg^{2+} titrations carried out to confirm the expected 2 : 1 stoichiometry.

1a. ^{1}H NMR (C_6D_6, 250 MHz, C_6D_5H = 7.30 ppm) 1.24–1.29 (m, 4H, THF-CH_2(3, 4)), 3.60–3.66 (m, 4H, THF-CH_2(2, 5)), 7.58 (tt, ^3J = 7 Hz, ^4J = 2 Hz, 2H, aryl-H(4)), 7.69 (dd, ^3J = 7 Hz, ^3J = 6 Hz, 4H, aryl-H(3, 5)), 8.30 (dd, ^3J = 6 Hz, ^4J = 2 Hz, aryl-H(2, 6)). A 2 : 1 THF/Ph_2Mg stoichiometry was found. The ^{1}H NMR spectrum of uncoordinated THF (same conditions) was recorded separately: 1.54–1.59 (m, 4H, THF-CH_2(3, 4)), 3.69–3.74 (m, 4H, THF-CH_2(2, 5)). ^{13}C NMR (toluene-d_8, 62.89 MHz, toluene aryl-H(4) = 125.6 ppm) 25.8 (t, ^1J = 135 Hz, 2C, THF-CH_2(3, 4)), 69.7 (t, ^1J = 149 Hz, 2C, THF-CH_2(2, 5)), 125.9 (d, ^1J = 156 Hz, 2C, phenyl-C(4)), 127.2 (d, ^1J = 153 Hz, 4C, phenyl-C(3)), 141.9 (d, ^1J = 151 Hz, 4C, phenyl-C(2)), 167.4 (s, 2C, phenyl-C(1)).

3. ^{1}H NMR (toluene-d_8, 250 MHz, tol. CD_2H = 2.32 ppm) 1.37–1.42 (m, 4H, THF-CH_2(3, 4)), 2.59 (s, 6H, Me), 3.67–3.72 (m, 4H, THF-CH_2(2, 5)), 7.52 (d (AB), ^3J = 7 Hz, 4H, aryl-H(3)), 8.24 (d(AB), ^3J = 7 Hz, 4H, aryl-H(2)). A THF: Ar_2Mg stoichiometry of about 1.7 was found. As a reference, the ^{1}H NMR spectrum of free THF (same conditions) was recorded: δ 1.66–1.72 (m, 4H, THF-CH_2(3, 4)), 3.75–3.80 (m, 4H, THF-CH_2(2, 5)). A concentrated solution of crystalline **1a** in toluene-d_8 (10 mm tube) was investigated by ^{17}O NMR spectroscopy on a Bruker MSL 400 spectrometer at a frequency of 54.2 MHz. ^{17}O NMR (toluene-d_8, ext. ref.

$D_2O = 0$ ppm) δ 11.4 (s, $\Delta\nu_{1/2} = 240$ Hz). The data for THF (20%) under the same conditions were: ^{17}O NMR (toluene-d_8, ext. ref. $D_2O = 0$ ppm) δ 16.7 (s, $\Delta\nu_{1/2} = 80$ Hz).

The diarylmagnesium compounds **1** and **3** were also prepared in diethyl ether, by the procedure described above. Addition of n-pentane (10 mL) to a solution of **3** (1 mmol) in diethyl ether (10 mL) resulted in a clear solution, which was concentrated to 3 mL, then cooled (10 °C). Colorless crystals were formed, but turned out to be unstable, immediately disintegrating in vacuum with loss of solvent of solvation.

3. ^1H NMR (THF-d_8, 250 MHz, ref. THF-$d_7 = 1.75$ ppm) δ 1.14 (t, $^3J = 7$ Hz, 6H, $Et_2O(Me)$), 2.21 (s, 6H, aryl-Me), 3.43 (q, $^3J = 7$ Hz, 4H, $Et_2O(CH_2)$), 6.85 (d(AB)d, $^3J = 7$ Hz, $^4J = 1$ Hz, 4H, aryl-H(3)), 7.60 (d(AB)d, $^3J = 7$ Hz, $^4J = 1$ Hz, 4H, aryl-H(2)). Most of the diethyl ether of solvation was lost during the isolation of the crystals from the mother liquor; an $Et_2O : Ar_2Mg$ stoichiometry of 0.32 was found. The complex is completely dissociated in THF, and the chemical shifts of the diarylmagnesium signals are identical to those previously reported [10].

In spite of several attempts, no Ph_2Mg diethyl etherate could be isolated; in all cases an oil was formed. A sample of this oil was dissolved in toluene-d_8 and the ^1H NMR spectrum (250 MHz) revealed an Et_2O to diarylmagnesium ratio of 2.5. When the temperature was lowered marked changes in the NMR spectrum were observed. 298 K: δ 1.07 (t, $^3J = 7$ Hz, 6H, CH_3), 3.42 (q, $^3J = 7$ Hz, 4H, CH_2), 7.53–7.59 (m, 6H, aryl-H(3,4)), 8.26 (bs, 4H, aryl-H(2)). 223 K: δ 1.07 (bs, 6H, CH_3), 3.41 (bs, 4H, CH_2), 7.63–7.81 (m, 6H, aryl-H(3,4)), 8.40 (bs, 4H, aryl-H(2)). 205 K: δ 1.10 (bs, 6H, CH_3), 3.44 (bs, 4H, CH_2), 7.54–7.72 (m, 2H, aryl-H(4)), 7.85 (t, $^3J = 7$ Hz, 4H, aryl-H(3)), 8.44 (d, $^3J = 7$ Hz, 4H, aryl-H(2)).

Solvent-free diphenylmagnesium (**1b**) was crystallized by use of a high dilution technique. A solution of **1** (20 mmol) in diethyl ether (200 mL), prepared as described above, was concentrated to a total volume of about 5 mL, and to this oily, yellowish-brown, residue was added a large quantity (2 L) of benzene, to give a clear solution. The solution was set aside for several months, during which crystals of **1b** slowly separated. The crystalline material (less than 1 mmol) was isolated, and remaining traces of solvent were removed by evacuation to 10^{-3} mbar. Some crystals were dissolved in THF-d_8, and the ^1H NMR spectrum showed that only diphenylmagnesium was present, with no trace of diethyl ether or benzene. The remaining crystals were transferred a nitrogen-filled glovebox, and crystals were selected for an X-ray structure determination.

X-ray crystallographic studies

Crystal data and details of the structure determinations are given in Table 1. Final atomic coordinates and equivalent isotropic thermal parameters are listed in Table 2 Neutral atom scattering factors were taken from [11] and corrected for anomalous dispersion [12]. All calculations were performed with SHELX76 [13] and the EUCLID package [14] (geometrical calculations and illustrations) on a MicroVAX cluster.

Structure determination and refinement of ***1a***. A colourless rod-shaped crystal was mounted under nitrogen in a Lindemann glass capillary and transferred to an Enraf-Nonius CAD4F diffractometer for data collection. Unit cell parameters were determined from a least squares treatment of the SET4 setting angles of 25 reflections and were checked for the presence of higher lattice symmetry [15]. Data

Table 1

Crystal data and details of the structure determinations

	1a	**3**	**1b**
(a) *Crystal data*			
Formula	$C_{20}H_{26}MgO_2$	$C_{36}H_{44}MgO_2 \cdot (C_{22}H_{30}MgO_2)_2$	$C_{12}H_{10}Mg$
Mol. wt.	322.73	1258.92	178.52
Crystal system	orthorhombic	triclinic	orthorhombic
Space group	*Fdd*2 (No. 43)	$P\bar{1}$ (No. 2)	*Imcb* (No. 72)
a, *b*, *c* (Å)	26.820(4) 19.781(3) 7.250(5)	11.40(1), 11.846(8), 16.091(6)	5.676(1) 9.614(3) 18.708(3)
α, β, γ (°)	–	68.76(4), 79.73(6), 73.88(7)	–
V (Å^3)	3846(3)	1938(3)	1020.9(4)
Z	8	1	4
D_{calc} (Mg m^{-3})	1.115	1.079	1.161
$F(000)$	1392	680	376
μ (cm^{-1})	8.2	7.8	1.2
Crystal size (mm)	1.38×0.25×0.20	0.95×0.43×0.20	0.5×0.3×0.2
(b) *Data collection*			
Temperature (K)	295	295	295
θ_{min}, θ_{max} (°)	1.65, 70.0	2.96, 70.0	1.08, 29.99
Radiation, λ (Å)	Cu-K_α (Ni-filtered), 1.54184	Cu-K_α (Ni-filtered), 1.54184	Mo-K_α (Zr-filtered), 0.71073
Scan type	$\omega/2\theta$	$\omega/2\theta$	$\omega/2\theta$
$\Delta\omega$ (°)	0.60+0.15 tan θ	0.55+0.15 tan θ	0.60+0.35 tan θ
Hor. and vert. aperture (mm)	3.0, 5.0	3.0, 5.0	3.0, 6.0
Dist. cryst. to detector (mm)	173	173	173
Reference reflections	−2 2 −2, −4 −2 0, −6 0 −2	−2 −1 3, 0 0 4	2 0 0, 0 0 2
Data set	*h* 0:32; *k* 0:24; *l* 0:8 (+Bijvoet-pairs)	*h* −13:0; *k* −14:14; *l* −19:19	*h* 0:7; *k* 0:13; *l* 0:26
Total data	3650	7746	877
Total unique data	1791	7350	815
Observed data	1119 [$I > 2.5\sigma(I)$]	2632 [$I > 2.5\sigma(I)$]	455 [$I > 2.5\sigma(I)$]
(c) *Refinement*			
No. of refined parameters	105	409	45
Weighting scheme	$w = 1.0/[\sigma^2(F)]$	$w = 1.0/[\sigma^2(F) = 0.000553F^2]$	$w = 1.0/[\sigma^2(F)]$
Final R, R_w, S	0.0547, 0.0528, 1.57	0.0707, 0.0766, 0.91	0.051, 0.046, 0.74
$(\Delta/\sigma)_{max}$ in final cycle	0.019	0.016	0.022
Min. max. resd. dens. (e/Å^3)	−0.31, 0.26	−0.26, 0.28	−0.21, 0.28

Table 2

Atomic coordinates and isotropic thermal parameters with esd's in parentheses for $Ph_2Mg \cdot [THF]_2$ (**1a**), $[Tol_2Mg]_3 \cdot [THF]_2$ (**3**) and $[Ph_2Mg]_n$ (**1b**)

Atom	x	y	z	U_{eq} [a] or U_{iso} (Å^2)
Compound 1a				
Mg	0	0	3/4	0.0762(6)
O(1)	0.0496(1)	0.0336(2)	0.9407(5)	0.107(1)
C(1)	−0.0277(2)	0.0865(2)	0.6087(5)	0.070(1)
C(2)	−0.0714(2)	0.0852(2)	0.5045(7)	0.091(2)
C(3)	−0.0864(2)	0.1383(3)	0.3900(8)	0.110(2)
C(4)	−0.0582(2)	0.1953(2)	0.3739(7)	0.105(2)
C(5)	−0.0154(2)	0.1993(2)	0.4723(9)	0.102(2)
C(6)	−0.0010(1)	0.1466(2)	0.5886(6)	0.088(2)
C(7)	0.0392(3)	0.0880(3)	1.0691(9)	0.170)3)
C(8)	0.0783(2)	0.0943(4)	1.182(1)	0.197(5)
C(9)	0.1183(2)	0.0490(4)	1.1301(9)	0.139(3)
C(10)	0.0956(2)	0.0032(3)	0.9903(9)	0.126(2)
Compound 3b				
Mg(1)	0.0820(2)	0.4625(2)	0.4317(1)	0.0691(8)
O(1)	0.0002(3)	0.4888(4)	0.3225(3)	0.089(2)
C(1)	0.0380(6)	0.6475(5)	0.4529(4)	0.079(3)
C(2)	−0.0463(6)	0.7551(6)	0.4076(4)	0.085(3)
C(3)	−0.0275(8)	0.8716(7)	0.3851(5)	0.108(3)
C(4)	0.075(1)	0.8932(8)	0.4038(6)	0.127(5)
C(5)	0.1617(8)	0.7897(9)	0.4469(5)	0.116(4)
C(6)	0.1436(6)	0.6725(7)	0.4703(4)	0.094(3)
C(7)	0.096(1)	1.0240(7)	0.3789(6)	0.214(6)
C(8)	−0.1199(6)	0.5590(6)	0.2968(5)	0.105(3)
C(9)	−0.1609(8)	0.4809(8)	0.2568(6)	0.151(5)
C(10)	−0.0558(8)	0.3840(9)	0.2468(7)	0.175(6)
C(11)	0.0458(8)	0.4023(8)	0.2732(6)	0.156(5)
C(12)	0.2670(5)	0.3650(6)	0.4139(4)	0.077(2)
C(13)	0.3678(6)	0.4191(6)	0.3852(4)	0.087(3)
C(14)	0.4875(6)	0.3506(8)	0.3744(4)	0.098(3)
C(15)	0.5147(7)	0.2257(8)	0.3913(4)	0.089(3)
C(16)	0.4185(7)	0.1691(6)	0.4186(4)	0.089(3)
C(17)	0.3007(6)	0.2363(6)	0.4300(4)	0.085(3)
C(18)	0.6448(6)	0.1517(7)	0.3805(5)	0.132(3)
Compound 3a				
Mg(2)	0.1892(2)	0.1110(2)	0.0316(1)	0.0874(9)
O(2)	0.2950(4)	0.1354(4)	0.1113(3)	0.100(2)
O(3)	0.2089(4)	−0.0755(4)	0.0928(3)	0.109(2)
C(19)	0.4244(7)	0.0848(8)	0.1186(6)	0.144(5)
C(20)	0.4639(9)	0.162(1)	0.1563(9)	0.220(7)
C(21)	0.3647(8)	0.2580(9)	0.1695(7)	0.157(5)
C(22)	0.2565(7)	0.2272(7)	0.1558(6)	0.126(4)
C(23)	0.0080(6)	0.2078(6)	0.0617(4)	0.081(3)
C(24)	−0.0831(7)	0.1619(6)	0.1231(4)	0.091(3)
C(25)	−0.2004(7)	0.2326(7)	0.1363(5)	0.095(3)
C(26)	−0.2338(6)	0.3550(8)	0.0883(5)	0.090(3)
C(27)	−0.1485(8)	0.4066(6)	0.0270(5)	0.106(3)
C(28)	−0.0313(7)	0.3335(7)	0.0144(5)	0.106(3)
C(29)	−0.3625(6)	0.4355(7)	0.1020(6)	0.137(4)

Table 2 (continued)

Atom	x	y	z	U_{eq} [a] or U_{iso} (Å^2)
Compound 3a				
C(30)	0.2832(5)	0.1484(5)	−0.0985(4)	0.079(3)
C(31)	0.2674(6)	0.1060(6)	−0.1656(6)	0.091(3)
C(32)	0.3252(7)	0.1376(7)	−0.2512(6)	0.101(4)
C(33)	0.4034(7)	0.2167(8)	−0.2781(5)	0.100(3)
C(34)	0.4199(6)	0.2610(6)	−0.2160(6)	0.096(3)
C(35)	0.3628(6)	0.2289(6)	−0.1309(5)	0.088(3)
C(36)	0.4667(8)	0.2525(9)	−0.3716(6)	0.172(5)
C(37)	0.277(1)	−0.1733(9)	0.0614(7)	0.181(6)
C(38)	0.271(1)	−0.2920(8)	0.1322(8)	0.180(6)
C(39)	0.185(1)	−0.258(1)	0.1985(9)	0.244(7)
C(40)	0.159(2)	−0.138(1)	0.172(1)	0.39(1)
Compound 1b				
Mg	1/4	0	0	0.0451(4)
C(1)	1/2	0.1297(3)	0.0665(2)	0.051(1)
C(2)	1/2	0.2716(3)	0.0499(2)	0.063(1)
C(3)	1/2	0.3753(5)	0.1006(3)	0.100(2)
C(4)	1/2	0.3381(6)	0.1707(3)	0.135(3)
C(5)	1/2	0.2012(6)	0.1908(2)	0.109(2)
C(6)	1/2	0.1007(4)	0.1394(2)	0.064(1)

[a] U_{eq} = 1/3 of the trace of the orthogonalized U matrix.

were collected within two Bijvoet-related quadrants of the reflection sphere and corrected for Lp, for a small linear decay (1.7%) of the intensities during the 44 h of X-ray exposure time but not for absorption. Data were merged into a unique dataset (R_{int} = 8.3%). The magnitudes of the standard deviations indicated by counting statistics were increased in the light of an analysis of the excess variance of the reference reflections: $\sigma^2(I) = \sigma_{cs}^2(I) + (0.021 \cdot I)^2$ [16]. The structure was solved by standard Patterson methods (SHELXS86 [17]) and a series of subsequent difference Fourier syntheses. Refinement on F was carried out by full matrix least squares techniques. H-atoms were introduced at calculated positions (C–H = 0.98 Å) and included in the refinement riding on their carrier atoms. All non-hydrogen atoms were refined with a common isotropic thermal parameter (U = 0.198(8) Å^2). Two low order reflections with $F_o \ll F_c$ were excluded from the final refinement stages. Weights were introduced in the final refinement cycles, convergence was reached at R = 0.0547. The absolute structure was checked by refinement with $-if''$ anomalous scattering factors resulting in R = 0.0563; R_w = 0.0554.

Structure determination of 3. A colourless plate shaped crystal was mounted under nitrogen in a Lindemann glass capillary and transferred to an Enraf-Nonius CAD4F diffractometer for data collection. Unit cell parameters were determined by a least squares treatment of the setting angles of 10 reflections with 11.7 < θ < 17.0°. The unit cell parameters were checked for the presence of higher lattice symmetry [15]. Data were corrected for Lp, for a small linear decay (1.4%) of the intensities during the 73 h of X-ray exposure time, and for absorption (DIFABS [18]; correction range: 0.57–1.43). The values of the standard deviations indicated by counting statistics were increased in the light of an analysis of the excess variance of the reference reflections: $\sigma^2(I) = \sigma_{cs}^2(I) + (0.012 \cdot I)^2$ [16]. The structure was solved by

direct methods (SHELXS86) and subsequent difference Fourier syntheses. Refinement on F was carried out by full matrix least squares techniques. H-atoms were introduced on calculated positions (C–H = 0.98 Å) and included in the refinement riding on their carrier atoms. All non-hydrogen atoms were refined with anisotropic thermal parameters, H-atoms were refined with three separate common isotropic thermal parameters. Weights were introduced in the final refinement cycles, convergence was reached at $R = 0.0707$.

Structure determination of 1b. A block shaped colourless crystal was mounted in a Lindemann glass capillary and transferred to an Enraf-Nonius CAD4F diffractometer for data collection. Unit cell parameters were determined from a least squares fit of the SET4 setting angles of 25 reflections with $8.3 < \theta < 17.5°$, and were checked for the presence of higher lattice symmetry [15]. Data were corrected for Lp, for a small linear decay (3%) of the intensities during the 13 h of X-ray exposure time and for absorption (DIFABS [18]; correction range 0.66–1.38). The magnitudes of the standard deviations indicated by counting statistics were increased in the light of an analysis of the excess variance of the three reference reflections: $\sigma^2(I) = \sigma_{cs}^2(I) + (0.013 \cdot I)^2$ [16]. The structure was solved by direct methods followed by peak optimization (SHELXS86 [17]). Refinement on F was carried out by full matrix least squares techniques (SHELX76 [13]). Hydrogen atoms were introduced at calculated positions (C–H = 0.98 Å) and included in the refinement riding on their carrier atoms. All non-hydrogen atoms were refined with anisotropic thermal parameters. Hydrogen atoms were refined with individual isotropic thermal parameters ($U = 0.06$–0.20 Å^2). Weights were introduced in the final refinement cycles; convergence was reached at $R = 0.051$.

Results and discussion

Compounds **1** and **3** were made from the corresponding diaryl-mercury compounds diphenylmercury (**4**) and bis(*p*-tolyl)mercury (**5**) [19]. After purification of **4** and **5**, high vacuum techniques were used in the exchange reaction with magnesium to exclude the presence of hydrolysis or oxidation products in the diarylmagnesium solution obtained. High purity of the diarylmagnesium solutions is essential, since impurities interfere in the crystallization process or even lead to isolation of undesired species. For this reason, the synthesis of **1** via symmetrization of phenylmagnesium bromide with *p*-dioxane is unsuitable [20]. THF solvates of both **1** and **3** were obtained by crystallization from a THF/n-hexane mixture. The identity of the crystals was checked by ^{1}H NMR spectroscopy (in C_6D_6 or toluene-d_8), and the amount of crystal solvent was estimated (found **1a**: 2.0 eq. THF: **3**: 1.7 eq. THF). Relative to the free ligand, the signals from the THF protons were shifted to high field upon complexation ($\Delta\delta$ − 0.30 ppm (α-CH_2), − 0.08 ppm (β-CH_2)).

The position of the ^{17}O NMR resonance signal for a concentrated solution of **1a** was determined, relative to that for free THF in toluene-d_8. The presence of Mg–O coordination is clearly indicated by broadening of the oxygen signal (from 80 to 240 Hz half width), relative to that for free THF. In contrast, the chemical shift difference between coordinated and free THF molecules was small in comparison with the 700 ppm shift range for ^{17}O NMR signals [21]: a 5.3 ppm shielding was observed. This makes ^{17}O NMR spectroscopy less suitable for studying the com-

Table 3

Bond distances (Å) and angles (°) for **1a**[a]

Mg–O(1)	2.030(4)	C(3)–C(4)	1.363(7)
Mg–C(1)	2.127(4)	C(4)–C(5)	1.355(8)
O(1)–C(7)	1.450(7)	C(5)–C(6)	1.395(6)
O(1)–C(10)	1.418(6)	C(7)–C(8)	1.34(1)
C(1)–C(2)	1.395(6)	C(8)–C(9)	1.45(1)
C(1)–C(6)	1.396(5)	C(9)–C(10)	1.490(9)
C(2)–C(3)	1.398(7)		
O(1)–Mg–O(1)′	94.2(1)	C(2)–C(1)–C(6)	112.9(3)
O(1)–Mg–C(1)	107.1(1)	C(1)–C(2)–C(3)	123.4(4)
O(1)–Mg–C(1)′	111.3(1)	C(2)–C(3)–C(4)	120.8(5)
O(1)′–Mg–C(1)	111.3(1)	C(3)–C(4)–C(5)	118.3(4)
C(1)–Mg–C(1)′	122.4(1)	C(4)–C(5)–C(6)	120.6(4)
Mg–O(1)–C(7)	123.7(4)	C(1)–C(6)–C(5)	123.9(4)
Mg–O(1)–C(10)	127.1(3)	O(1)–C(7)–C(8)	108.2(6)
C(7)–O(1)–C(10)	108.6(5)	C(7)–C(8)–C(9)	111.4(7)
Mg–C(1)–C(2)	122.7(3)	C(8)–C(9)–C(10)	104.5(5)
Mg–C(1)–C(6)	123.8(3)	O(1)–C(10)–C(9)	105.7(5)

[a] ′ indicates symmetry operation $-x, -y, z$.

plexation of organomagnesium compounds with ether ligands, contrary to our initial expectation.

Crystal structures of the THF adducts of 1 and 3

The THF adducts of both **1** and **3** were studied by X-ray diffraction. In the case of **1**, a normal pseudo-tetrahedral complex $Ph_2Mg \cdot [THF]_2$ (**1a**) was found, in which the diarylmagnesium unit is coordinated by two THF molecules. Bond distances and angles are listed in Table 3. The crystallization of **3** yielded a remarkable double structure, in which separate molecules of $(p\text{-tolyl})_2Mg(THF)_2$(monomer, **3a**) and $[(p\text{-tolyl})_2MgTHF]_2$ (dimer, **3b**) co-crystallized in a 2 : 1 ratio. The presence of two independent organomagnesium species in one unit cell is a relatively rare phenomenon, although other examples are known [22]. Several factors which may give rise to this can be considered. In the first place, under our conditions of crystallization of **3**, the two aggregates may have comparable thermodynamic stabilities; the low THF concentration in n-hexane is expected to play a role. In addition, favorable packing of **3a** and **3b** in the unit cell of the crystal apparently helps to bring both components of the association equilibrium together into one crystal. The bond lengths and angles of **3** are listed in Tables 4 and 5, respectively.

The structures of the monomeric complexes **1a** and **3a** are closely related, as can be seen from Fig. 1. The simularity between the structures is evident from Table 6. The bond distances (Mg–C 2.126(7)–2.132(8) Å, Mg–O 2.030(4)–2.050(5) Å) lie in the normal range for organomagnesium compounds. The coordination geometry around the central magnesium atom deviates from tetrahedral, with a larger C–Mg–C angle (**1a**: 122.4(1)°; **3a** 124.4(3)°) and a smaller O–Mg–O angle (**1a**: 94.2(1)°; **3a** 96.7(2)°). These features are common in organomagnesium chemistry, and are found in many crystal structures of such compounds [23]. So far, only one simple diarylmagnesium complex has been structurally characterized viz. $Ph_2Mg \cdot$ TMEDA

Table 4

Bond distances (Å) for 3

Compound 3b					
Mg(1)–O(1)	2.020(5)	C(2)–C(3)	1.36(1)	C(12)–C(13)	1.40(1)
Mg(1)–C(1)	2.245(7)	C(3)–C(4)	1.37(2)	C(12)–C(17)	1.40(1)
Mg(1)–C(1)''	2.313(7)	C(4)–C(5)	1.38(1)	C(13)–C(14)	1.40(1)
Mg(1)–C(12)	2.130(7)	C(4)–C(7)	1.53(1)	C(14)–C(15)	1.36(1)
O(1)–C(8)	1.435(8)	C(5)–C(6)	1.37(1)	C(15)–C(16)	1.37(1)
O(1)–C(11)	1.45(1)	C(8)–C(9)	1.51(1)	C(15)–C(18)	1.51(1)
C(1)–C(2)	1.406(9)	C(9)–C(10)	1.44(1)	C(16)–C(17)	1.38(1)
C(1)–C(6)	1.41(1)	C(10)–C(11)	1.40(1)		
Compound 3a					
Mg(2)–O(2)	2.050(5)	C(21)–C(22)	1.45(1)	C(31)–C(32)	1.38(1)
Mg(2)–O(3)	2.031(6)	C(23)–C(24)	1.38(1)	C(32)–C(33)	1.38(1)
Mg(2)–C(23)	2.132(8)	C(23)–C(28)	1.39(1)	C(33)–C(34)	1.35(1)
Mg(2)–C(30)	2.126(7)	C(24)–C(25)	1.39(1)	C(33)–C(36)	1.51(1)
O(2)–C(19)	1.44(1)	C(25)–C(26)	1.35(1)	C(34)–C(35)	1.37(1)
O(2)–C(22)	1.44(1)	C(26)–C(27)	1.36(1)	C(37)–C(38)	1.47(2)
O(3)–C(37)	1.41(1)	C(26)–C(29)	1.54(1)	C(38)–C(39)	1.40(2)
O(3)–C(40)	1.34(2)	C(27)–C(28)	1.40(1)	C(39)–C(40)	1.30(2)
C(19)–C(20)	1.46(1)	C(30)–C(31)	1.40(1)		
C(20)–C(21)	1.41(2)	C(30)–C(35)	1.40(1)		

(**6**) [24]. Some differences between the structure of **6** and **1a** or **3a** can be associated with the nature of the TMEDA ligand. The coordinative bonds in **6** are longer (Mg–N 2.205(3) and 2.199(3) Å), while the N–Mg–N angle is smaller (82.5(1)°) because of the formation of a five-membered chelate ring. These structural features are also present in the crystal structure of the related complex $Me_2Mg \cdot$ TMEDA (**7**) [25].

The crystal structure of the centrosymmetric complex **3b** (Fig. 2) represents the first for a dimeric simple diarylmagnesium compound. Bridging μ-*p*-tolyl groups in **3b** connect both metal centres via three-center two-electron bonds. In the central four-membered Mg_2C_2 ring, two different metal–carbon bond distances can be seen (Mg(1)–C(1) 2.245(7) Å, Mg(1)–C(1)′ 2.313(7) Å). The central ring is rhomboidal, with large C–Mg–C angles (102.5(2)°) and small Mg–C–Mg angles (77.5(2)°). This leads to a relatively short Mg–Mg distance (2.853(4) Å), which compares with a bonding distance of 2.76 Å (from Mg–C = 2.15 Å) and a contact distance in magnesium metal of 3.2 Å [9]. Although the distance might suggest the possibility of some direct metal-metal bonding, we think this is unlikely. The bridging of the aryl groups is unsymmetrical; the short Mg–C bond is closer to the plane of the aryl ring than the longer bond (angles: 28.3(3) and 46.4(3)°, respectively). In addition, the bridging aryl groups are twisted out of a symmetrical perpendicular position (see Fig. 3), and this reduces the angle between the planes Mg_2C_2 and C(1–7) from 90 to 76.2(3)°. This brings an *ortho*-carbon atom close to a magnesium atom, and introduces some η^2-character into the bonding of the bridging aryl group (Mg(1)–C(2)′ 2.979(7) Å, Mg(1)–C(6) 3.052(9) Å). Each magnesium atom carries a terminal aryl group and a THF molecule, the bond lengths are normal (Mg(1)–O(1) 2.020(5) Å, Mg(1)–C(12) 2.130(7) Å). The positions of the terminal groups can be related to those of the bridging aryl groups. The planes of Mg_2C_2 and of the two *p*-tolyl

Table 5

Bond angles (°) for 3 [a]

Compound 3b			
O(1)–Mg(1)–C(1)	106.9(2)	C(3)–C(4)–C(7)	122.7(9)
O(1)–Mg(1)–C(1)′	102.6(2)	C(5)–C(4)–C(7)	121(1)
O(1)–Mg(1)–C(12)	106.9(2)	C(4)–C(5)–C(6)	121.1(9)
C(1)–Mg(1)–C(1)′	102.5(2)	C(1)–C(6)–C(5)	123.5(7)
C(1)–Mg(1)–C(12)	120.9(3)	O(1)–C(8)–C(9)	103.8(6)
C(1)′–Mg(1)–C(12)	115.3(3)	C(8)–C(9)–C(10)	107.3(8)
Mg(1)–O(1)–C(8)	129.7(4)	C(9)–C(10)–C(11)	108.6(9)
Mg(1)–O(1)–C(11)	119.3(5)	O(1)–C(11)–C(10)	107.3(8)
C(8)–O(1)–C(11)	108.4(6)	Mg(1)–C(12)–C(13)	125.3(5)
Mg(1)–C(1)–Mg(1)′	77.5(2)	Mg(1)–C(12)–C(17)	122.6(5)
Mg(1)–C(1)–C(2)	125.9(5)	C(13)–C(12)–C(17)	112.1(6)
Mg(1)–C(1)–C(6)	111.1(5)	C(12)–C(13)–C(14)	122.9(7)
Mg(1)′–C(1)–C(2)	103.8(5)	C(13)–C(14)–C(15)	122.4(7)
Mg(1)′–C(1)–C(6)	120.6(4)	C(14)–C(15)–C(16)	116.7(8)
C(2)–C(1)–C(6)	113.5(6)	C(14)–C(15)–C(18)	122.1(7)
C(1)–C(2)–C(3)	122.4(7)	C(16)–C(15)–C(18)	121.2(8)
C(2)–C(3)–C(4)	122.8(8)	C(15)–C(16)–C(17)	121.0(7)
C(3)–C(4)–C(5)	116.6(9)	C(12)–C(17)–C(16)	124.9(7)
Compound 3a			
O(2)–Mg(2)–O(3)	96.7(2)	C(24)–C(25)–C(26)	121.3(7)
O(2)–Mg(2)–C(23)	104.6(3)	C(25)–C(26)–C(27)	117.5(8)
O(2)–Mg(2)–C(30)	106.6(2)	C(25)–C(26)–C(29)	122.4(7)
O(3)–Mg(2)–C(23)	110.3(3)	C(27)–C(26)–C(29)	120.1(8)
O(3)–Mg(2)–C(30)	110.2(2)	C(26)–C(27)–C(28)	120.2(7)
C(23)–Mg(2)–C(30)	124.4(3)	C(23)–C(28)–C(27)	124.8(7)
Mg(2)–O(2)–C(19)	126.9(5)	Mg(2)–C(30)–C(31)	125.8(5)
Mg(2)–O(2)–C(22)	124.4(5)	Mg(2)–C(30)–C(35)	123.4(5)
C(19)–O(2)–C(22)	107.6(6)	C(31)–C(30)–C(35)	110.6(6)
Mg(2)–O(3)–C(37)	128.8(5)	C(30)–C(31)–C(32)	124.3(7)
Mg(2)–O(3)–C(40)	129.4(6)	C(31)–C(32)–C(33)	121.8(8)
C(37)–O(3)–C(40)	101.8(8)	C(32)–C(33)–C(34)	115.8(7)
O(2)–C(19)–C(20)	105.5(8)	C(32)–C(33)–C(36)	122.3(8)
C(19)–C(20)–C(21)	110.7(9)	C(34)–C(33)–C(36)	121.8(8)
C(20)–C(21)–C(22)	105.3(9)	C(33)–C(34)–C(35)	122.2(7)
O(2)–C(22)–C(21)	108.5(7)	C(30)–C(35)–C(34)	125.2(7)
Mg(2)–C(23)–C(24)	128.7(5)	O(3)–C(37)–C(38)	108.6(9)
Mg(2)–C(23)–C(28)	119.4(5)	C(37)–C(38)–C(39)	104(1)
C(24)–C(24)–C(28)	111.8(7)	C(38)–C(39)–C(40)	106(1)
C(23)–C(24)–C(25)	124.4(7)	O(3)–C(40)–C(39)	119(1)

[a] ′ indicates symmetry operation: $-x, 1-y, 1-z$.

groups C(1–7) and C(12–18) tend more towards coplanarity (see Fig. 3; C(1–7)–C(12–18) 34.4(3)°, Mg_2C_2–Mg(1)–C(12) 41.0(2)°), than the Mg(1)–O(1) bond, which tends to be more perpendicular to the Mg_2C_2 plane (65.9(2)°). The unsymmetrical bridging of the *p*-tolyl groups in **3b** can be related to the fact that the magnesium carries two different terminal substituents. The bridging *p*-tolyl groups tends towards greater coplanarity with the terminal ones; in contrast the phenyl groups in **1b** bridge in a symmetrical manner between the magnesium atoms because these are bonded to two identical groups.

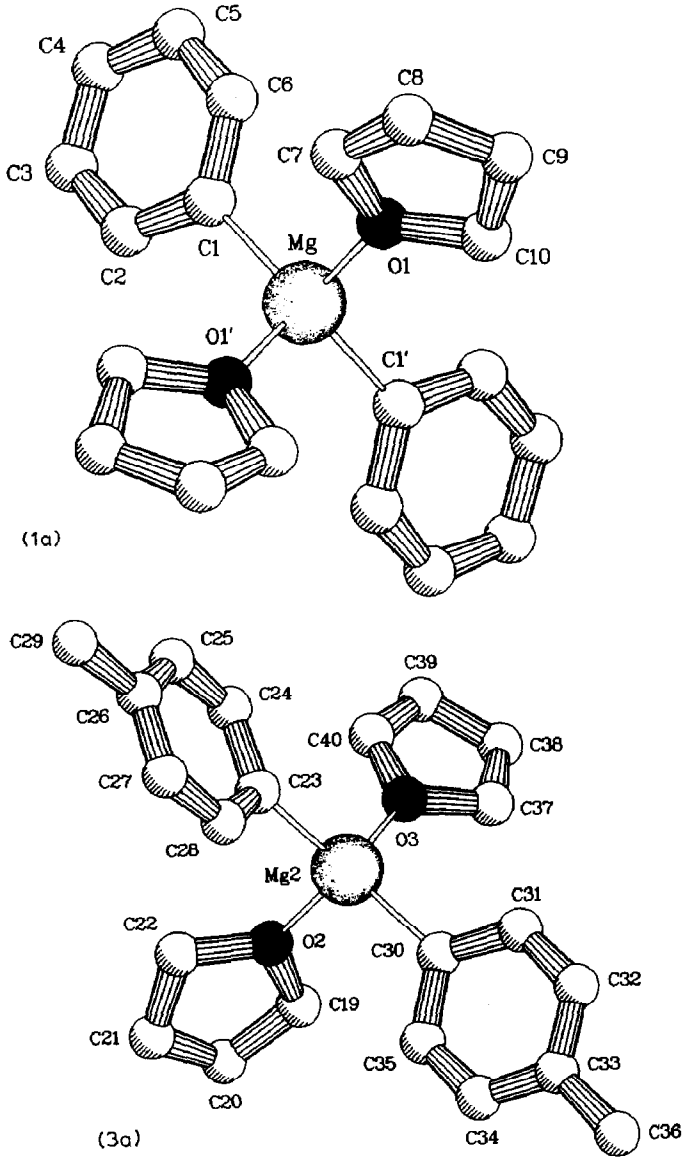

Fig. 1. PLUTON drawing of the monomers $Ph_2Mg \cdot [THF]_2$ (**1a**) and $(p\text{-tolyl})_2Mg \cdot [THF]_2$ (**3a**), in similar projections; hydrogen atoms omitted for clarity.

Bridging aryl groups between two magnesium atoms are also found in the magnesate complex $[Ph_2Mg \cdot PhLi \cdot TMEDA]_2$ (**8**) [26]. The centrosymmetric four-membered Mg_2Ar_2 rings in the central part of structures **3b** and **8** have much in common. In both species, the bridging of the aryl group is unsymmetrical, giving rise to two different Mg–C bond lengths (**8**: 2.286(3) and 2.329(3) Å). The intraannular C–Mg–C and Mg–C–Mg angles in **8** also have values comparable with those for **3b** (102.1(7) and 77.3(3)°, respectively). In both structures, the magnesium atom with the shortest Mg–C distance is closer to the plane of the bridging phenyl group than the other magnesium atom (**8**: −1.18 and 1.68 Å, respectively). In

Table 6

Comparison of important bond distances (Å) and angles (°) in **1a** and **3a**

$Ph_2Mg \cdot [THF]_2$ (**1a**)		$[Tol_2Mg] \cdot [THF]_2$ (**3a**)	
Mg–C(1)	2.127(4)	Mg(2)–C(23)	2.132(8)
		Mg(2)–C(30)	2.126(7)
Mg–O(1)	2.030(4)	Mg(2)–O(2)	2.050(5)
		Mg(2)–O(3)	2.031(6)
C(1)–Mg–C(1)′	122.4(1)	C(23)–Mg(2)–C(30)	124.4(3)
O(1)–Mg–O(1)′	94.2(1)	O(2)–Mg(2)–O(3)	96.7(2)
O(1)–Mg–C(1)	107.1(1)	O(2)–Mg(2)–C(23)	104.6(3)
		O(2)–Mg(2)–C(30)	106.6(2)
O(1)′–Mg–C(1)	111.3(1)	O(3)–Mg(2)–C(23)	110.3(3)
		O(3)–Mg(2)–C(30)	110.2(2)

contrast to those in **3b**, the planes of the four-membered Mg_2Ph_2 ring and the bridging phenyl group in **8** are almost perfectly perpendicular (89.5°). This may be related to the more symmetrical environment of the magnesium atoms in **8** (four phenyl groups), compared with those in **3b**, which bear two different terminal groups (*p*-tolyl and THF).

Diethyl ether adducts

As mentioned in the Experimental section, the isolation of stable diethyl ether adducts from **1** or **3** was not possible owing to loss of crystal solvent. This behavior must be attributed to the weaker coordinative ability of diethyl ether than of THF. From association measurements, it is known that diorganylmagnesium compounds are monomeric in THF over a large concentration range, and probably have a

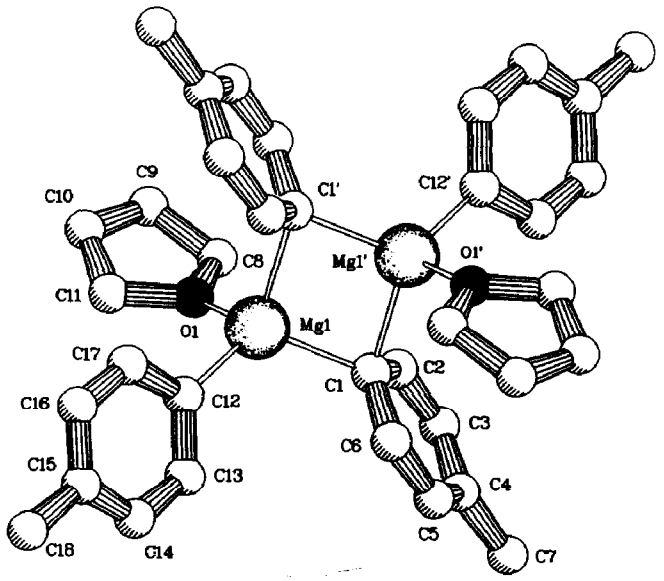

Fig. 2. PLUTON drawing of the dimer $[(p\text{-tolyl})_2Mg \cdot THF]_2$ (**3b**); hydrogen atoms are omitted for clarity.

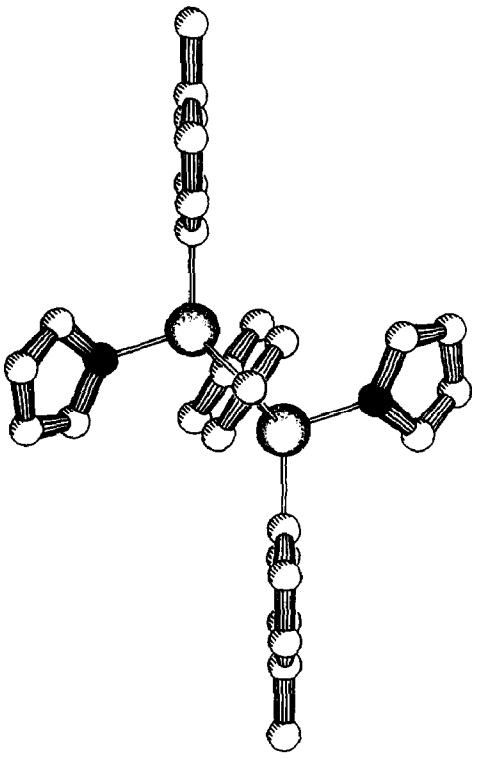

Fig. 3. PLUTON drawing of $[(p\text{-tolyl})_2Mg \cdot THF]_2$ (**3b**), showing the relative orientation of the bridging phenyl groups relative to the Mg_2C_2 four-membered ring.

structure in solution analogous to that of **1a** and **3a** [27]. On the other hand, in diethyl ether, the association increases at higher concentrations. For **1**, an association degree of 1.8 is reached in a 1.5 *M* solution in pure diethyl ether. These results clearly demonstrate the limited coordinating power of diethyl ether, which in competition with μ-aryl groups is too weak to prevent oligomerization at higher concentrations. The variable temperature ^1H NMR spectra of **1** along with 2.5 eq. of diethyl ether in toluene-d_8 showed the following effects at lower temperatures (see Experimental section): (i) The signals of the broad phenyl-H multiplet sharpened, and eventually a partial interpretation became possible; (ii) The positions of the phenyl-H signals shifted to lower field, and eventually became identical to those of **1a** in C_6D_6; (iii) The diethyl ether signals, a triplet (CH_3) and a quartet (CH_2) at room temperature, changed to broad signals without fine structure. These results can be accounted for in terms of the dissociation equilibria between $Ph_2Mg \cdot [Et_2O]_2$ and its oligomers (see Scheme 1). The equilibria shift to the right at lower temperature, and eventually almost all the diphenylmagnesium will be present as monomeric $Ph_2Mg \cdot [Et_2O]_2$. The broadening of the phenyl-H signals due to dynamic processes disappears, and the spectrum of the monomeric diethyl ether complex essentially resembles that of **1a**. The broadening of the diethyl ether signals is a consequence of the slowing down of the exchange between complexed and free (excess) diethyl ether at lower temperatures. From the relative thermodynamic stability of the monomer at lower temperatures, it must be concluded that it has a

lower enthalpy than the associated species, i.e. the Mg–O bond is more stable than the bridging phenyl group.

Polymeric diphenylmagnesium (1b).

Crystallization of **1b** was from a highly dilute solution in benzene containing a trace of diethyl ether (see Experimental section). The very low solubility of **1b** in this medium facilitates its crystallization, shifting the equilibrium of Scheme 1 to the left. In order to obtain crystals suitable for a X-ray structure determination, this process must be very slow. The crystals obtained were identified by ^{1}H NMR spectroscopy in THF-d_8 as pure $[Ph_2Mg]_n$, without any solvent of crystallization (diethyl ether or benzene). Compound **1b** has a polymeric structure with a high degree of symmetry (Fig. 4). This feature may simplify future theoretical calculations on the structure of **1b**. Relevant data on the structure of **1b** can be found in Table 7. The tetra-coordinated magnesium atoms are arranged in a linear chain in the *a*-direction (Mg–Mg 2.8380(9) Å) and connected by symmetrically bridging phenyl groups via three-center two-electron bonds (Mg–C 2.261(2) Å, Mg–C–Mg 77.73(9)°). The centrosymmetric four-membered Mg_2C_2 rings are joined approximately perpendicular to each other (89.83(15)°). An analysis of the thermal motion shows libration of the chain around its axis. The coordination geometry of the magnesium atoms deviates from tetrahedral owing to the presence of the four-membered Mg_2C_2 rings. Three different C–Mg–C angles are found: 102.27(7)° inside the ring and 113.08(9) and 113.3(1)° outside.

The crystal structure of **1b** is the first for a polymeric diorganylmagnesium. The growth of single crystals of such species from apolar solvents is extremely difficult,

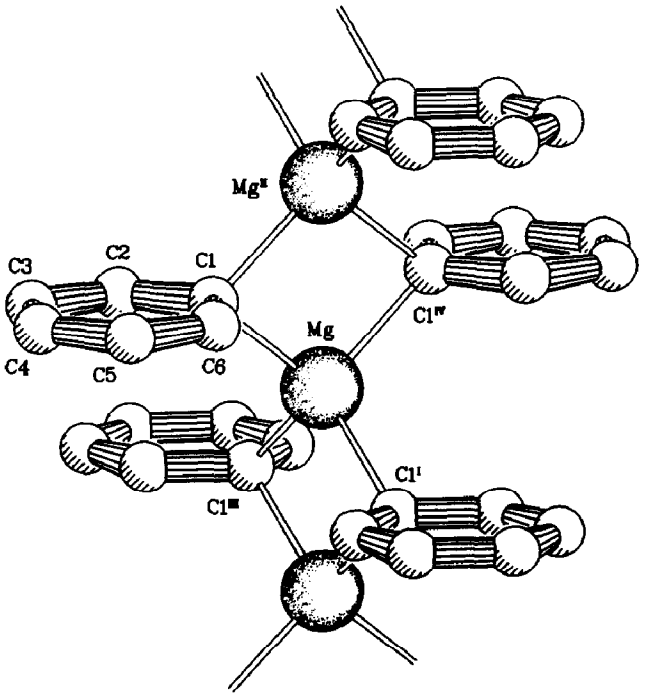

Fig. 4. PLUTON drawing of the $[Ph_2Mg]_n$ structure (**1b**) with adopted labeling showing part of the infinite chain in the *a*-direction.

Table 7

Bond distances (Å) and angles (°) for **1b**[a]

Mg(1)–C(1)	2.261(2)		
C(1)–C(2)	1.399(4)	C(3)–C(4)	1.359(8)
C(1)–C(6)	1.394(5)	C(4)–C(5)	1.369(8)
C(2)–C(3)	1.376(6)	C(5)–C(6)	1.362(6)
Mg–C(1)–C(2)	114.6(2)	C(2)–C(3)–C(4)	118.3(4)
Mg–C(1)–C(6)	115.4(2)	C(3)–C(4)–C(5)	121.2(5)
C(2)–C(1)–C(6)	114.3(3)	C(4)–C(5)–C(6)	119.2(4)
C(1)–C(2)–C(3)	123.6(4)	C(1)–C(6)–C(5)	123.3(4)
Mg–C(1)–Mg^{ii}	77.73(9)	C(1)–Mg–C(1)^{iv}	102.27(7)
C(1)–Mg–C(1)^{i}	113.3(1)	C(1)–Mg–C(1)^{iii}	113.08(9)

[a] Symmetry code: (*i*) $x-1/2, -y, z$; (*ii*): $x+1/2, -y, z$; (*iii*): $x-1/2, y, z$; (*iv*): $-x, -y, -z$.

as these reagents normally have a very low solubility because of their polymeric nature. This renders the growth of good quality single crystals almost impossible. For the simple dialkylmagnesium reagents $[Me_2Mg]_n$ (**9**) and $[Et_2Mg]_n$ (**10**), the structure was determined by powder diffraction techniques [5]. These structures are comparable to those of **1b**, with the alkyl groups symmetrically bridging between the magnesium atoms. Unfortunately, powder diffraction techniques are not suitable for more complicated structures. In future investigations, the high dilution technique applied for **1b** may also be useful to give crystals of other unsolvated diorganylmagnesium compounds suitable for single crystal studies.

We previously reported the crystal structure of the unsolvated adduct $[NpMgBr \cdot Np_2Mg]_n$ (**11**) [28]. This neopentylmagnesium compound has an exceptionally high solubility in apolar solvents, which facilitates normal crystallization from a n-heptane/toluene mixture. The structure of **11** consists of a polymeric chain with a backbone of tetracoordinated magnesium atoms, analogous to **1b**, **9** and **10**. In an alternating sequence of 1 : 3, the magnesium atoms are connected by two μ-Br or two μ-CH_2CMe_3 groups. A higher symmetry for **11** is probably prevented by the nature of the neopentyl group, which has a low bridging ability owing to higher steric hindrance, and by the perturbing effect of the halogen atoms; these effects combine to lead to the presence of recognizable substructures of the components NpMgBr and Np_2Mg, in a sort of memory effect.

Acknowledgement

X-ray data for **1b** and **3** were kindly collected by A.J.M. Duisenberg. This work was supported in part (P.R.M., W.J.J.S., A.L.S.) by The Netherlands Foundation for Chemical Research (SON) with financial aid from The Netherlands Organization for Scientific Research (NWO).

Supplementary material available. Anisotropic thermal parameters, H-atom parameters, lists of bond lengths, bond angles, torsion angles, an ORTEP plot for **1b**, and lists of observed and calculated structure factor amplitudes (61 pages) are available from A.L.S.

References

1 P.R. Markies, T. Nomoto, O.S. Akkerman, F. Bickelhaupt, W.J.J. Smeets, A.L. Spek, J. Am. Chem. Soc., 110 (1988) 4845.
2 P.R. Markies, T. Nomoto, O.S. Akkerman, F. Bickelhaupt, W.J.J. Smeets, A.L. Spek, Angew. Chem., 100 (1988) 1143.
3 G.E. Coates, J.A. Heslop, J. Chem. Soc., A, (1966) 26.
4 G. Westera, G. Schat, C. Blomberg, F. Bickelhaupt, J. Organomet. Chem., 144 (1978) 273.
5 E. Weiss, J. Organomet. Chem., 2 (1964) 314; E. Weiss, ibid., 4 (1965) 101.
6 A.D. Vreugdenhil, C. Blomberg, Recl. Trav. Chim. Pays-Bas, 82 (1963) 453.
7 J.L. Wardell, in J.L. Wardell (Ed.), Organometallic Compounds of Zinc, Cadmium and Mercury, Chapman and Hall, London/New York.
8 K.E. Rowland, R.D. Thomas, Magn. Res. Chem., 23 (1985) 1985.
9 CRC Handbook of Chemistry and Physics, 60th ed.: R.C. Weast, M.J. Astle (Ed.), CRC Press Inc.
10 A. Villena, Thesis, Free University, Amsterdam, 1986.
11 D.T. Cromer, J.B. Mann, Acta Crystallogr. A, 24 (1968) 321.
12 D.T. Cromer, D. Liberman, J. Chem. Phys., 53 (1970) 1891.
13 G.M. Sheldrick, SHELX76. Crystal structure analysis package, Univ. of Cambridge, England, 1976.
14 A.L. Spek, The EUCLID Package in Computational Crystallography, D. Sayre (Ed.), Clarendon Press, Oxford, 1982, p. 528.
15 A.L. Spek, J. Appl. Cryst., 21 (1988) 578.
16 L.E. McCandlish, G.H. Stout, L.C. Andrews, Acta Crystallogr., A, 31 (1975) 245.
17 G.M. Sheldrick, SHELXS86. Program for crystal structure determination, Univ. of Göttingen, Federal Republic of Germany, 1986.
18 N. Walker, D. Stuart, Acta Cryst. A, 39 (1983) 158.
19 W. Schlenk, Chem. Ber., 64 (1931) 736.
20 W. Strohmeier, Chem. Ber., 88 (1955) 1218.
21 W.G. Klemperer, in J.B. Lambert, F.G. Riddel (Eds.), The Multinuclear Approach to NMR Spectroscopy, NATO ASI series C 103 (1982), Ch. 11, D. Reidel, Dordrecht.
22 T. Alonso, S. Harvey, P.C. Junk, C.L. Raston, B.W. Skelton, A.H. White, Organometallics, 6 (1987) 2110; P.C. Junk, C.L. Raston, B.W. Skelton, A.H. White, J. Chem. Soc., Chem. Commun., (1987) 1162.
23 W.E. Lindsell, in G. Wilkinson, F.G.A. Stone and E.W. Abel (Eds.), Comprehensive Organometallic Chemistry, Pergamon Press, Oxford, 1982, p. 155.
24 D. Thoennes, E. Weiss, Chem. Ber., 111 (1978) 3381.
25 T. Greiser, J. Kopf, D. Thoennes, E. Weiss, J. Organomet. Chem., 191 (1980) 1.
26 D. Thoennes, E. Weiss, Chem. Ber., 111 (1978) 3726.
27 E.C. Ashby, Bull. Soc. Chim. Fr., (1972) 2133.
28 P.R. Markies, G. Schat, O.S. Akkerman, F. Bickelhaupt, W.J.J. Smeets, A.L. Spek, J. Organomet. Chem., 375 (1989) 11.